

Supplementary Online Materials (SOM)

SOM #1. Qualitative knowledge on IL-2r regulation in T_{eff} and T_{reg} cells

SOM #2. Validating the estimates of surface IL-2R α and IL-2R β levels by flow cytometry.

SOM #3. Validation of the antibody against pSTAT5 for Flow cytometer measurements.

SOM #4. Individual curves for the dependency of pSTAT5 response to IL-2 with IL-2R α and IL-2R β levels.

SOM #5. pSTAT5 response to IL-2 is the same for T_{reg} and T_{eff} cells.

SOM #6. Parameters and validity of the two step model for IL-2/IL-2r binding.

SOM #7. Short time scale IL-2 depletion assay.

SOM #8. Autocrine vs Paracrine regulation for the IL-2 cytokine.

SOM #9. Experimental validation of the well-mixed approximation for IL-2

SOM #10. Exogenous IL-2 reverses the effect of T_{reg} cells in an α CD3/ α CD28 suppression assay.

SOM #11. “The double hit”: T_{reg} cells abrogate IL-2 binding by T_{eff} cells by reducing both IL-2 concentrations and IL-2R α levels in T_{eff} cells under activation with α CD3/ α CD28 cross-linking.

SOM #12. “The double hit”: T_{reg} cells abrogate IL-2 binding by T_{eff} cells by reducing both IL-2 concentrations and IL-2R α levels in T_{eff} cells under antigen activation.

SOM# 13. Pre-exposure to IL-2 *in vivo* increases T_{reg} cells suppression *in vitro*.

SOM #14. 48 hr regimen of IL-2 *in vivo* does not increase the size of the T_{reg} pool.

SOM #15. Diminished proliferation after IL-2 injections *in vivo* is not the result of diminished antigen-presenting and activation capabilities by CD4⁺ splenocytes.

SOM #16. Adoptive transfer of IL-2 treated (compared to PBS-treated) T_{reg} cells is sufficient to limit T_{eff} cell proliferation *in vivo*.

SOM References.

SOM #1. Qualitative knowledge on IL-2r regulation in T_{eff} and T_{reg} cells

Here we review qualitative understanding on IL-2/IL-2r regulation as is summarized in Figure 1. Naïve T cells present tonic low levels of IL-2R β and IL-2R γ (CD122 and CD132), do not present IL-2R α (CD25) and do not express IL-2. Upon antigen activation, naïve T cells differentiate into T_{eff} cells that upregulate their IL-2R α levels and secrete IL-2 within a few hours. Upregulation of IL-2R α leads to the formation of the high-affinity IL-2r trimer (IL-2R α , IL-2R β & IL-2R γ) that is functionally active. Upon sensing IL-2 (in an autocrine or paracrine fashion), IL2 production is suppressed (Kim *et al*, 2006; Kim *et al*, 2001; Villarino *et al*, 2007) but IL-2R α expression is enhanced (Kim *et al*, 2006). Bound IL-2 is endocytosed and degraded and thus depleted from the environment (Duprez and Dautry-Varsat, 1986).

As far as the response of T cells to IL-2 upon engagement of their IL-2R is concerned, both thermodynamic measurements of the IL-2/IL-2r interaction at the molecular level (Rickert *et al*, 2005; Wang and Smith, 1987; Wu *et al*, 1999; Wu *et al*, 1995) and population average measurements (Smith, 1988; Takeshita *et al*, 1992; Wang *et al*, 1987) estimate the affinity of the IL-2/IL-2r interaction to be constant at 10pMolar. However, studies at the single cell level revealed that T cell cycle progression is variable depending on the IL-2r surface density (Cantrell and Smith, 1984; Smith, 1988), which itself depends on the differentiation state of T cells.

T_{reg} cells, (defined as CD4⁺Foxp3⁺), constitutively express IL-2R β and IL-2R γ , but also intermediate levels of IL-2R α (10⁴/cell at steady state). They never express nor secrete any IL-2 molecules (de la Rosa *et al*, 2004). However, the potential to assemble the high affinity trimeric IL-2 receptor endows these cells with the ability to scavenge IL-2 that T_{eff} cells are secreting (Barthlott *et al*, 2005; Sojka *et al*, 2005). Thus, T_{reg}-mediated cytokine depletion has been suggested to be an important mechanism explaining T cell suppression (Barthlott *et al*, 2005; de la Rosa *et al*, 2004; Pandiyan *et al*, 2007)

SOM #2. Validating the estimates of surface IL-2R α and IL-2R β levels by flow cytometry.

We used flow cytometry to correlate IL-2R α and IL-2R β levels with pSTAT5 response within individual cells. Three controls needed to be performed:

- 1) Check that staining for IL-2R α and IL-2R β yields consistent results, despite potential receptor downregulation and degradation.

We checked that the staining for IL-2R α and IL-2R β were not affected by the 10min-exposure to IL-2 (Figure SOM #2A). Hence, despite potential epitope modification (e.g. upon glycosylation, phosphorylation or clustering), while pSTAT5 levels increase with time (Figure SOM #2A, left panel) IL-2r stainings remained constant (Figure SOM #2A, central and right panel) and validated as measurement of IL-2R α or IL-2R β levels within the cells.

- 2) Check that all receptors are membrane-bound at time 0.

To compare experimental results with our computer model (Figure 2E), we needed to check that measuring IL-2R α and IL-2R β levels by intracellular staining (we expect some of the receptors to be internalized after 10min of exposure to IL2) yielded an accurate estimate of the total number of available surface receptors at time 0. For that purpose, we stained live 5C.C7 T cell blasts after exposure to IL-2 with antibodies against IL-2R α and IL-2R β , fixed and permeabilized the cells and then restained for IL-2R α and IL-2R β . The linearity of the intracellular and extracellular staining (Figure SOM #2B, red lines with a slope of 1 are presented as a guide to the eye) and the results from the previous paragraph validate that, within a normalization factor, our measurement of IL-2R α and IL-2R β by intracellular staining yields accurate estimates of the number of available receptors at time 0.

- 3) Estimate of the absolute amount of IL-2R α & IL-2R β on the surface of cells.

To estimate the absolute amount of receptors on the surface of the cells, we used calibration beads (Bangs Labs, Fishers, IN) that are loaded with known amounts of PE dye. We calibrated the relationship between fluorescence and dye number in our FACS measurements (Figure SOM #2C-E), in order to convert or antibody staining for IL-2R α and IL-2R β into absolute number (assuming that the ratio of dye to antibody is 1/2 as specified by the manufacturer). Beads at five different fluorescence levels were used for calibration. The number of Fluorophores per bead is reported with the arrows above each respective peak in the FACS profile (Φ being blank beads).

The naïve CD4⁺ population from a wild type mouse (B10A) are presented in Figure SOM #2C. IL-2R α levels on T_{reg} cells (the 10% of CD25⁺ population –see dashed red arrow) center around 10,000 receptors per cell with high expressors approaching 10 times that amount. IL-2R β levels on the entire CD4⁺ population are below 1,000 copies per cell. Receptor levels on naïve B10.A CD4⁺ splenocytes (dashed red arrow in Figure

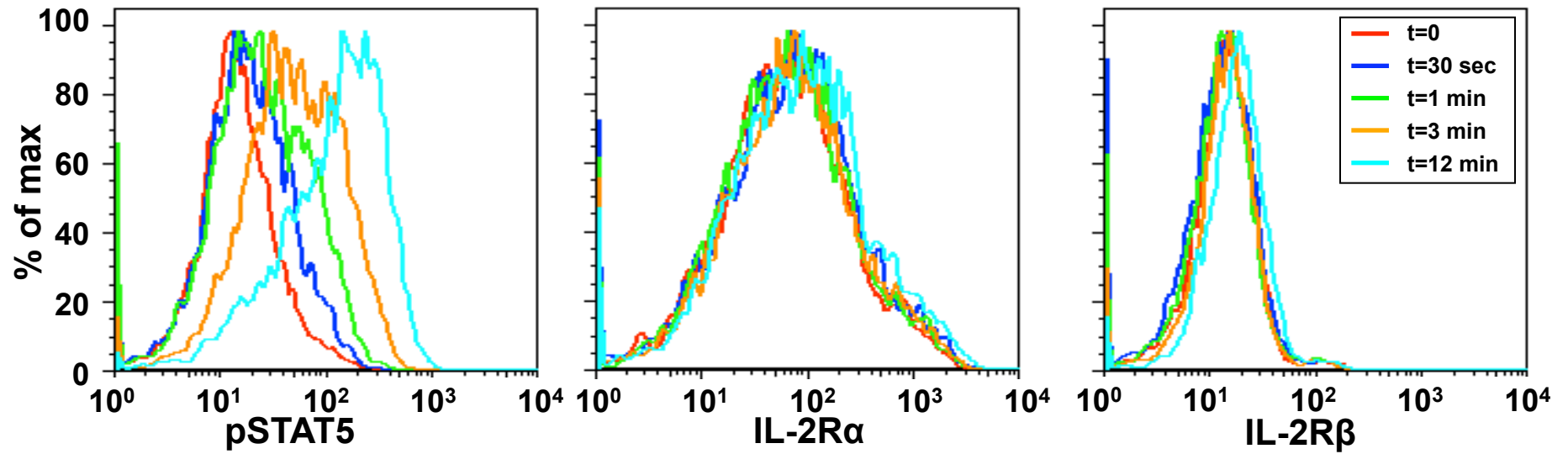
SOM #2C) or on naïve 5C.C7 TCR transgenic Rag2^{-/-} cells (Figure SOM #2D) have undetectable (overlapping with the isotype control) levels of less than 1000 and 400 IL-2R α receptors per cell respectively, IL-2R β levels are centered around 700 copies per cell. Figure SOM #2E shows FACS histograms of receptor levels on T cell blasts (5C.C7 cells 72 hours after stimulation with 1 μ M of K5 pulsed onto B10.A[CD3 ϵ ^{-/-} splenocytes) IL-2R α levels are centered around 60,000 copies per cell with high expressors with more than 350,000 copies per cell (48 hours after strong stimulation this number can get as high as a million copies per cell). IL-2R β levels center around 700 receptors per cell with high expressors at 10,000 copies per cell.

Figure SOM #2F specifies the two dimensional distribution of the absolute numbers of IL-2R α and IL-2R β (copies per cell) as calibrated from the MFI distributions given in Figure 2A. This distribution was used for the simulation presented in Figure 2B – theory and SOM #6. The color code is in logarithmic scale for the cell number per bin.

Note that there exists an apparent discrepancy between the bimodal distribution in Fig. 3A of Busse et al.'s paper (Busse et al, 2010), and the unimodal distribution we are reporting here in Fig. 2A and figure SOM #2F. This is most likely due to a difference in activation conditions and in measurement timescales between the two studies.

Figure SOM #2

A



B

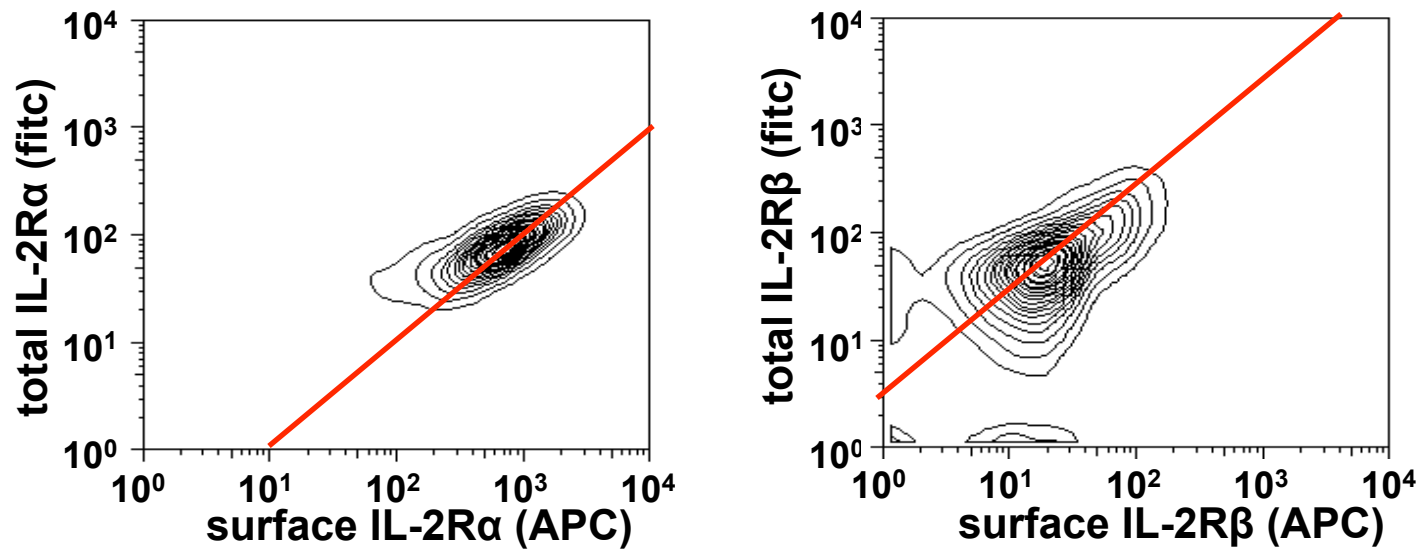
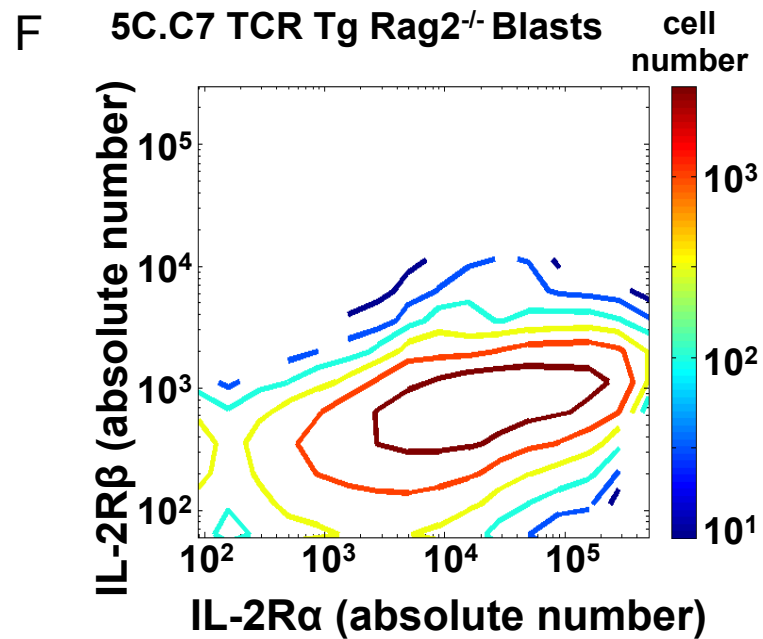
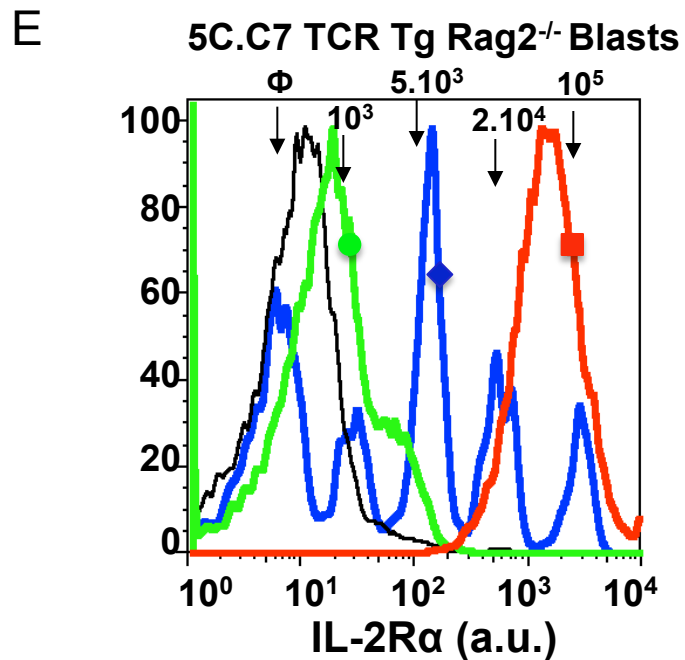
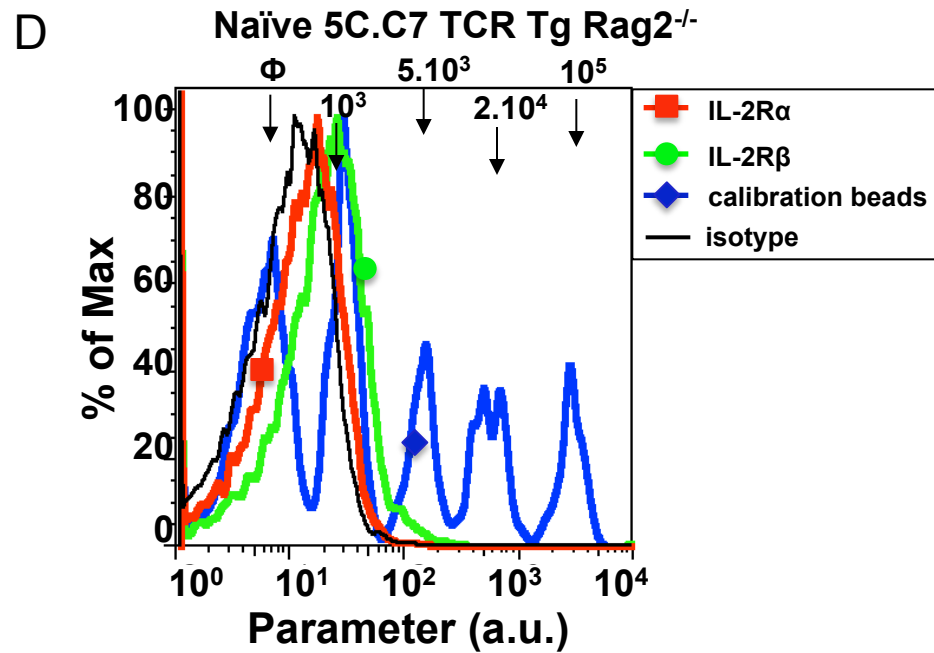
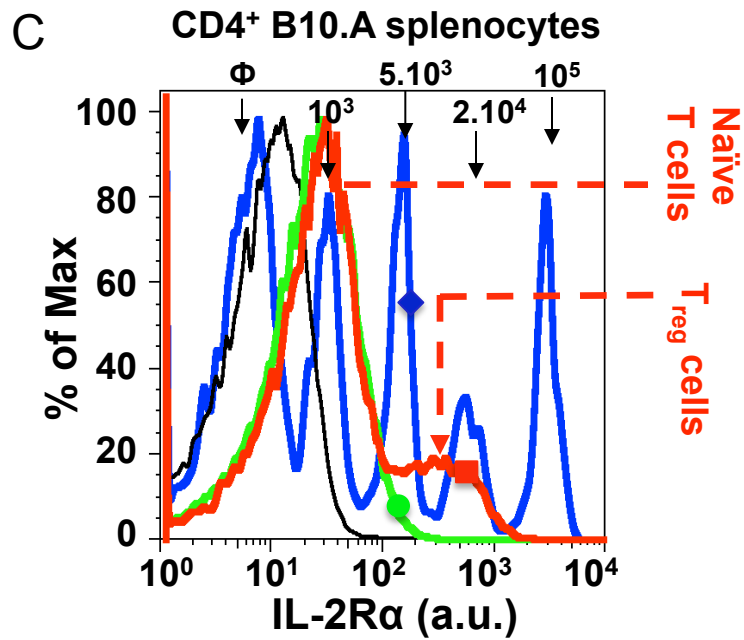


Figure SOM #2 (continued)



SOM #3. Validation of the antibody against pSTAT5 for flow cytometry measurements.

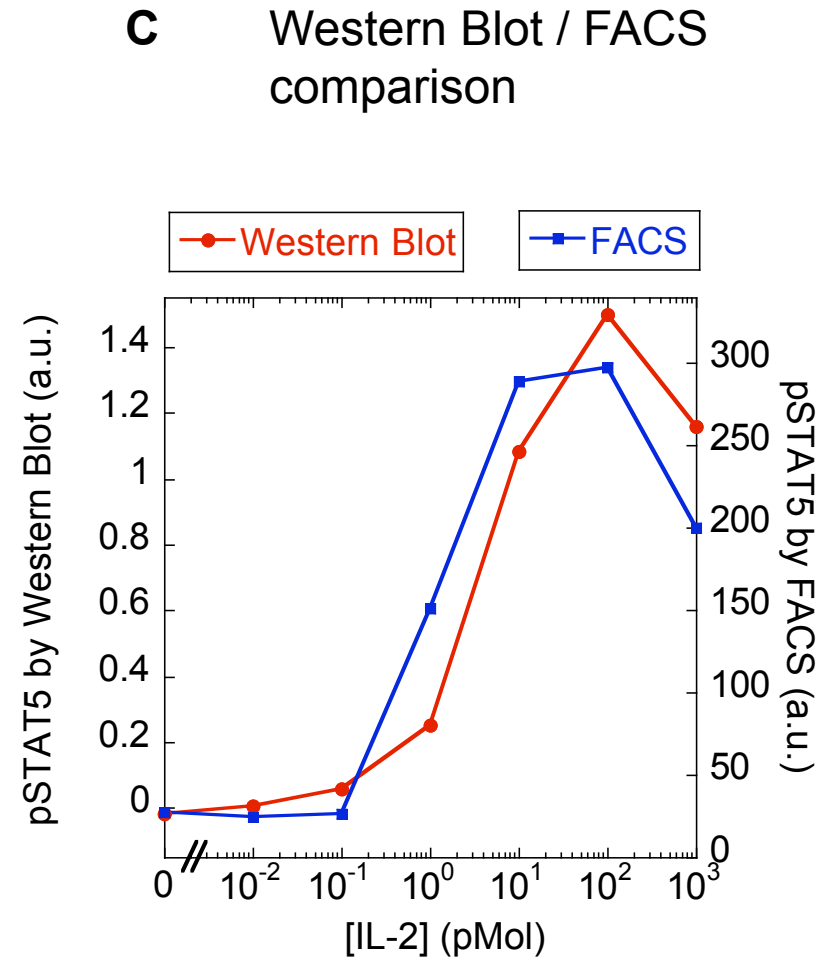
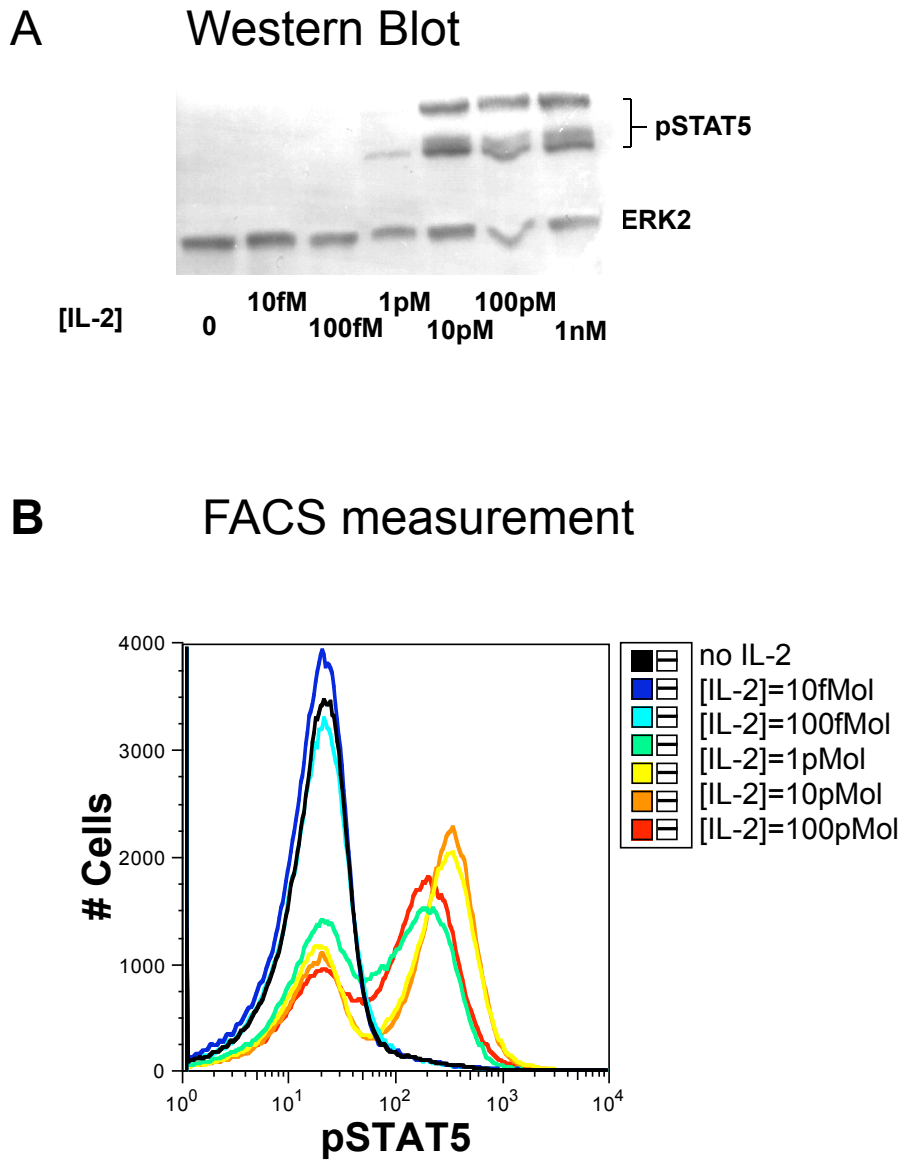
Following our methodology presented in (Feinerman *et al*, 2008), we performed measurements to validate the use of our antibody against phospho-STAT5 on Tyrosine 694 (clone C11C5 from Cell Signaling Technology –Danvers MA). Our validation consists in checking the consistency of pSTAT5 staining as measured on individual cell (by flow cytometry) and on a population of cells (by western blot). The western blot adds the molecular weight resolution that confirms the specificity of the pSTAT5 staining.

We used pre-activated 5C.C7 T cells (3 Days post-stimulation) that were spun on a Ficoll gradient to remove dead cells, and stripped of their IL-2 with a 2min-exposure to a low-pH buffer (0.1M Glycine, pH4.0) and washed in complete RPMI. Cells were then exposed to a serial dilution of mouse IL-2 (from 1nMol down to 10fMol) for 10min at 37°C and processed. Half of the samples was fixed with 1.6% paraformaldehyde for 10min on ice and permeabilized/stained according to protocol. The other half was lysed in 1%NP40 lysis buffer (complemented with protease inhibitor, sodium vanadate and iodoacetamide to inhibit phosphatases) for 30min on ice. Lysates were cleared from debris, denatured in SDS loading buffer at 99°C for 5min separated onto a 8% polyacrylamide denaturing gel. The gel was transferred onto a PVDF membrane, that was then immunoblotted with two rabbit antibodies against pSTAT5 (clone C11C5 from Cell Signaling Technology –Danvers MA) and ERK2 (polyclonal C-14 – Santa Cruz Biotechnology - Santa Cruz CA) as a loading control, and revealed with an anti-Rabbit antibody coupled with horseradish peroxydase.

The membrane was then incubated with peroxydase substrate (ThermoScientific Pierce, Waltham, MA), and exposed to X-ray film (Kodak, Rochester NY) –See Figure SOM #3A. The bands on the membrane were measured quantitatively using ImageJ (NIH, Bethesda MD): pSTAT5 was detected as a 95kDa-band and (monomer) a 190kDa-band (dimer) while ERK2 was detected as a 42kDa band.

In parallel, we measured pSTAT5 levels by flow cytometry (Figure SOM #3B). We then compared (Figure SOM #3C) the dose response to IL-2 by Western Blot to the linear average over pSTAT5 as measured by Flow Cytometry. The good agreement between the two curves validates the use of flow cytometry and single-cell measurement for pSTAT5.

Figure SOM #3



SOM #4. Individual curves for the dependency of pSTAT5 response to IL-2 with IL-2R α and IL-2R β levels.

Here we present the dot plots of pSTAT5 for different levels of IL-2R α and IL-2R β at each concentration of IL-2. This analysis was used to obtain the results presented in Figure 2B. Note how cells expressing high levels of IL-2R α are the most sensitive (with detectable pSTAT5 response at 1pMol) while cells expressing lower levels of IL-2R α need 10pMol or more to register any STAT5 phosphorylation (Figure SOM #4A). In Figure SOM #4B, we find that it is the absolute amplitude of the response that varies with IL-2R β levels. In Figure SOM #4C, we present a complete coverage of all IL-2/pSTAT5 dose-response, for all the IL-2R α and IL-2R β levels (corresponding to the experiment presented in Figure 2C).

Figure SOM #4

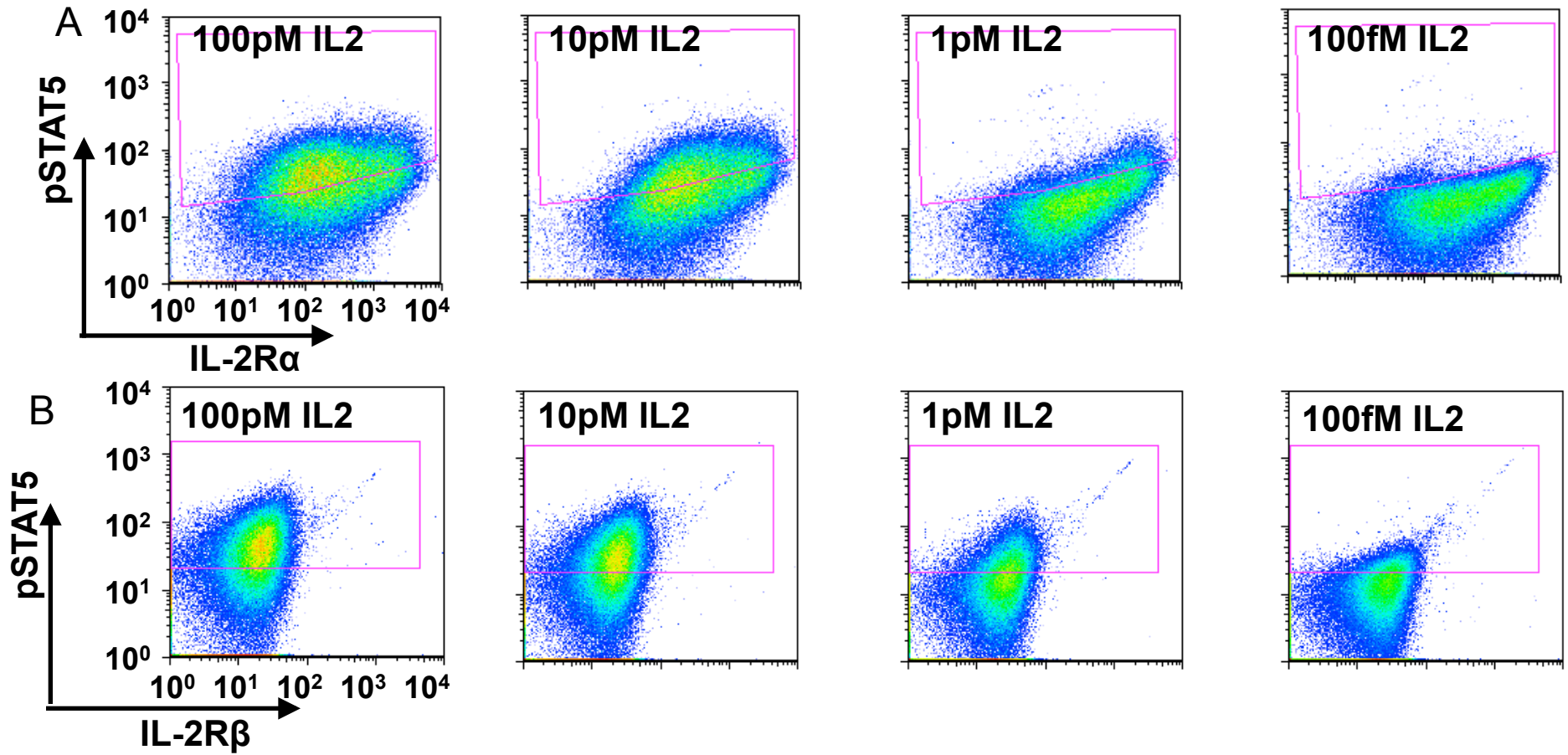
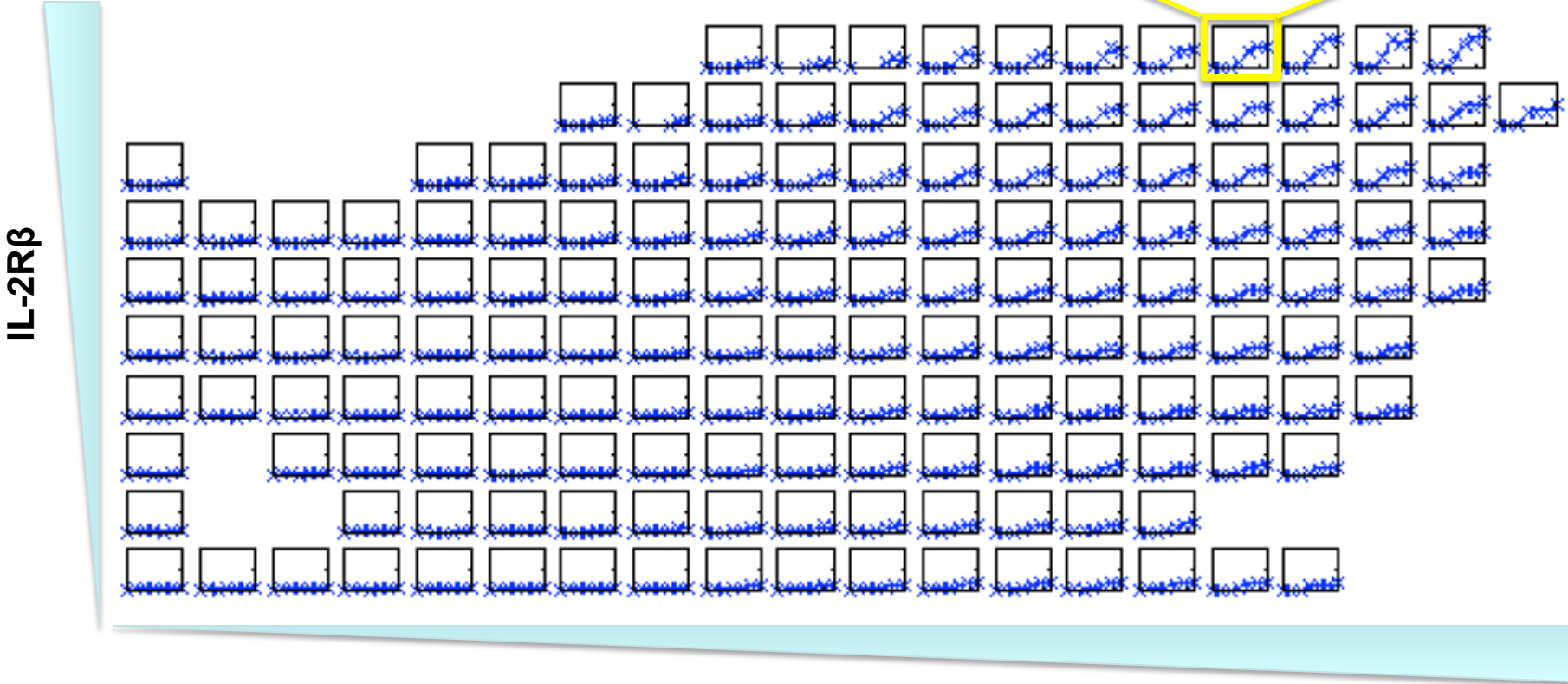
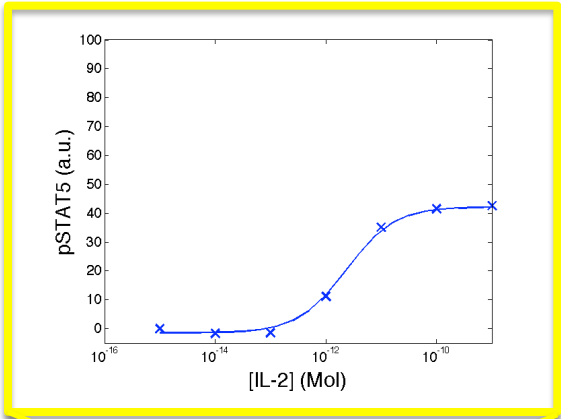


Figure SOM #4 (continued)

C



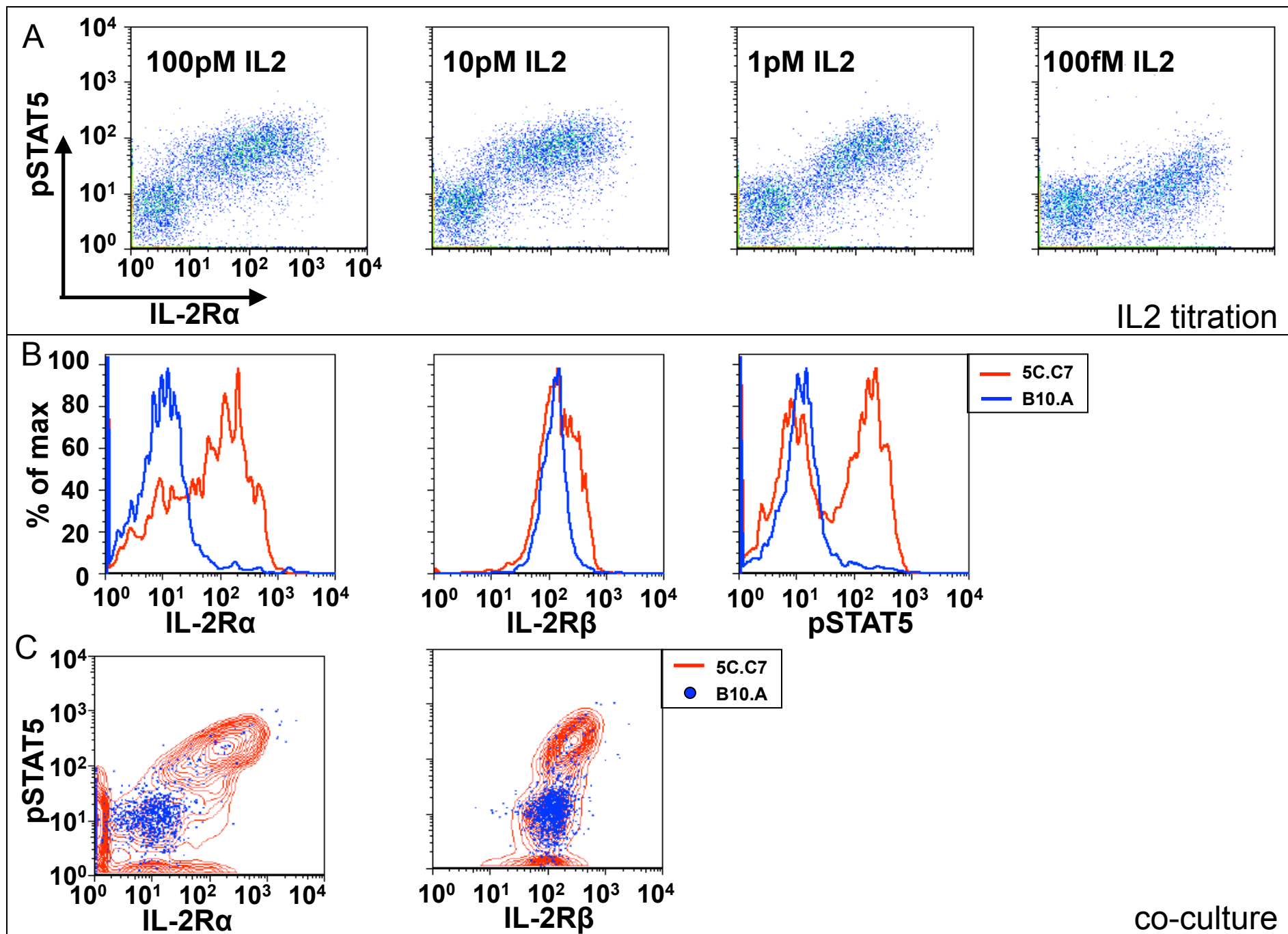
IL-2R α

SOM #5: pSTAT5 response to IL-2 is the same for T_{reg} and T_{eff} cells.

We tested whether our biochemical model for IL-2 binding and signaling to pSTAT5 (validated with our experiments on T_{eff} cell blasts) would be valid for T_{reg} cells. Naïve B10.A splenocytes were cultured for two days in the presence of 1nMolar IL2 to obtain a T_{reg} cell population with a wide IL-2R α distribution. Cells were then exposed to an IL2 titration following the same protocol used to obtain the results in Figure 2. Response of CD25⁺ cells to IL2 titration as a function of their IL-2R α levels is given in Figure SOM #5A and is highly similar to effector cell response (as in SOM Figure #3A). Costaining for IL-2R α and Foxp3 we find that over 85% of IL-2R α positive cells are indeed Foxp3 positive.

To confirm that the response of the two cell types is indeed identical we compared IL-2r and pSTAT5 level in co-cultured 5C.C7 (effector cells, CFSE stained) and B10.A cells (including a T_{reg} population). 5C.C7 cells were stimulated by 10nMolar of K5 and measurements were performed 35 hours later. The distribution of IL-2R α , IL-2R β and pSTAT5 levels in the B10.A and 5C.C7 CD4⁺ populations is extremely different (Figure SOM #5B). Thus, the comparison between the pSTAT5 responses of the two population must be done on a per-cell basis. Indeed, the dependency of STAT5 phosphorylation on IL-2R α and IL-2R β levels in both T_{eff} and T_{reg} cells is identical (Figure SOM #5C). Hence, T_{reg} and T_{eff} cells (despite their different differentiation states) trigger comparable STAT5 phosphorylation upon exposure to IL-2. This concordance simplifies the competition rules that we document in our study.

Figure SOM #5



SOM #6. Parameters and validity of the two step model for IL-2/IL-2r binding.

We obtained three of the model's parameters, the "off" rates for the IL-2/ IL2R α complex and the full IL-2/IL-2r complex as well as the "on" rate of the IL-2/IL2R α interaction (see Figure 2E) from previous direct measurements (Liparoto *et al*, 2002; Wang and Smith, 1987; Wang *et al*, 2005). The absolute IL-2 receptor subunit levels in Figure 2A were calibrated to give a maximum of $5 \cdot 10^5$ IL2R α receptors and a mode of approximately 10^3 IL2R β receptors per cell (see SOM #2). The "on rate" of the surface interaction has not been previously measured so we used it here as a free parameter adjusted to fit the experimental STAT5 phosphorylation on single cells (Figure 2B-exp. and 2B-theory) .

We compared a two-step mode (Figure 2E) to a three-step process in which IL2 binds to IL2R α , this dimer diffuses on the cell's surface to bind to IL2R β and form a trimer that then binds to IL2R γ to form the full stable signaling complex. The stability of the IL2/IL2R α /IL2R β complex ($k_{\text{off}}=0.02 \text{ s}^{-1}$ Liparoto, S.F. *et al*. (Liparoto *et al*, 2002) makes the formation of tetramers from trimers a non-limiting step. Indeed, modeling this interaction with rapid and concomitant IL2R β and IL2R γ binding, as we have done for simplicity's sake, changes the model predictions only slightly (EC_{50} s by a maximum of 25% and amplitudes by a maximum of 4% over the whole IL-2R α and IL-2R β expression range). This point is stressed throughout the manuscript by referring to IL-2R β /IL-2R γ instead of a IL-2R β •IL-2R γ complex. Furthermore, the binding of IL-2R β to IL-2R γ is not enough to induce pSTAT5 signaling as it relies on a conformational change induced by IL2 binding (Ellery and Nicholls, 2002).

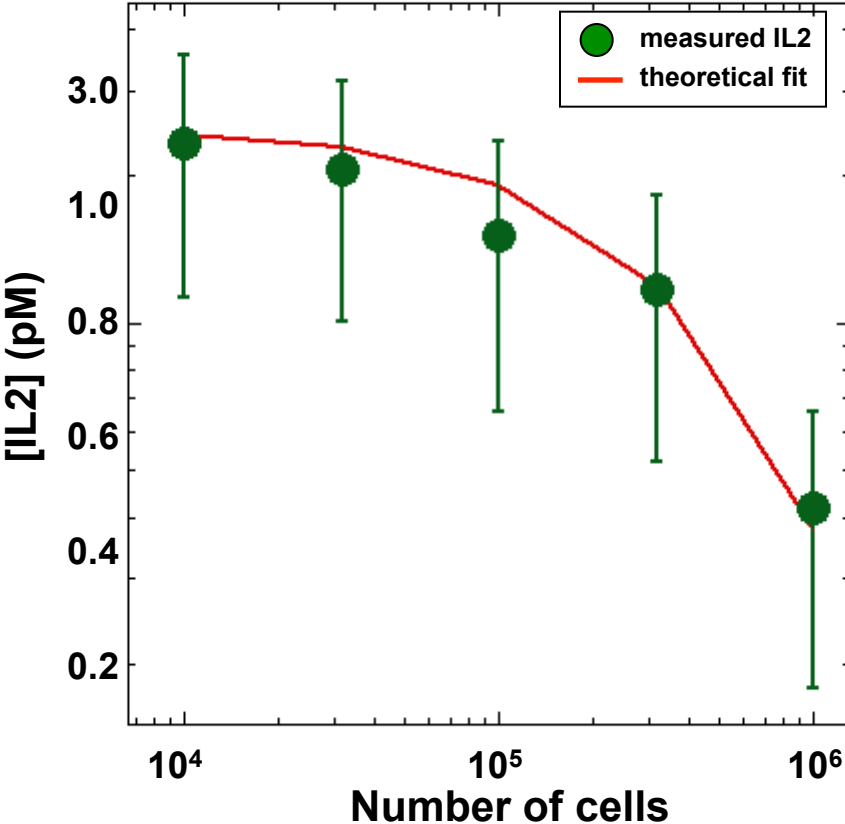
The model explains 84.2% of the variation in EC_{50} s ($p < 10^{-26}$ for correlation). While this number is not affected by randomly shuffling IL-2R β values (IL-2R β levels do not control EC_{50}) it goes down to 0% if the same is done for IL-2R α . This means that EC_{50} 's are mainly controlled by IL-2R α . Note that the classical model for IL-2/IL-2r interaction with a constant affinity constant at 10pMol would explain 0% of the variation in EC_{50} . The model explains 88% of the amplitude variation ($p < 10^{-33}$). Shuffling IL-2R β values the model explains only 76% of experimental variation in amplitudes. This correlation is again lost upon shuffling IL-2R α values, even though there is a weaker dependence of amplitude on IL-2R α the huge variability in the expression level of this subunit makes the effect of shuffling it more significant.

Note that a recent microscopic study of IL-2 binding on the surface of living cells demonstrated that IL-2R β and IL-2R γ were preassembled before binding IL-2 (Pillet *et al*, 2010). This experimental finding strongly supports our model of two-step binding kinetics for IL-2 on the surface of primary T cells.

SOM #7. Short time scale IL-2 depletion assay.

5C.C7 cells were cultured with irradiated B10.A cells in the presence of 1 μ Molar of the agonist K5. At d+2 dead cells were separated on a Ficoll gradient and live CD4⁺ 5C.C7 T cells collected. Cells were then acid stripped by IL-2, washed and rested for 10 minutes at 37°C. Different numbers of cells (10⁴-10⁶) were then exposed to 2.5pM of IL-2 for 10 minutes in 120 μ l after which supernatants were collected for subsequent measurement of IL-2 by ELISA. Results were fitted (by fine tuning IL-2R β levels) using the biochemical model with the measured distribution of IL-2R α and IL-2R β on the naïve CD4⁺CD25⁺ cells.

Figure SOM #7



SOM #8. Autocrine vs Paracrine regulation for the IL-2 cytokine.

Based on our experimental results (Figures 6A), our model for our experimental system relies on paracrine signaling and quorum sensing for T cell regulation. However, a recent model by (Busse *et al*, 2010) argued that autocrine signaling may play the predominant role in regulating T cell activation. Beyond our direct measurements on the density-dependence for pSTAT5 response that dismiss the autocrine mode of regulation (Figure 6A), we present here theoretical arguments to assess how IL-2 dependent regulation of T cells *in vitro* takes place.

1) Lack of autocrine loops: a theoretical argument

Stanislav Y. Shvartsman and coworkers have developed a theoretical framework for calculating the probability that an endogenous ligand will bind to the same cell from which it has been secreted. Their theory applies to our experimental setup as they model cell culture assays in which a dispersion of cells on the surface of a dish is covered by a layer of liquid medium (Batsilas *et al*, 2003). Moreover, they present an expression for calculating the cumulative probability $P(r)$ that a ligand will bind to another cell within a distance of r of its site of secretion.

Interestingly, the autocrine binding probability $P_{auto-binding}$ neither depends on the height of the medium nor on the amount of cells in the culture. Instead, $P_{auto-binding}$ is given by:

$$P_{auto-binding} = \frac{Da}{Da + 4/\pi},$$

which only depends on the dimensionless Damköhler number given by:

$$Da = k_{on} R_{total} / (\pi r_{cell} N_A D_L),$$

with k_{on} being the ligand-receptor binding rate constant. R_{total} marks the total number of receptors on a cell with radius r_{cell} , D_L accounts for the diffusion coefficient of the ligand and N_A is Avogadro's number. Using the parameters of our model,

$$k_{on} = 1.4 \times 10^7 M^{-1} s^{-1},$$

$$D_L = 100 \mu m^2 s^{-1} \text{ (Economou and Shin, 1978),}$$

$$\text{and } r_{cell} = 5 \mu m,$$

we estimate that, for weakly activated cells with 10^4 receptors, $Da=0.15$ and $P_{auto-binding}$ is approximately 0.10. For strongly activated cells with 10^5 receptors this values change to 1.5 and approximately 0.54 respectively.

However, binding in an autocrine loop does not warrant signaling in our IL-2 system under consideration. Indeed, the above theory yields an estimate for the probability of IL-2 molecules binding weakly to an α receptor subunit on the same cell that secreted it. To obtain a signaling complex the receptor ligand complex has to further bind to the $\beta\gamma$ subunit. Thus, the autocrine signaling probability $P_{auto-signal}$ is much reduced compared to the estimated $P_{auto-binding}$ above. To calculate the autocrine signaling probability we have to multiply the autocrine *binding* probability with the probability that a receptor ligand complex will bind to a $\beta\gamma$ subunit and lock into a full signaling complex. The probability to form a complete signaling complex is given by the

expression $\frac{k_{\beta\gamma}(\#mol_{\beta\gamma})}{k_{\beta\gamma}(\#mol_{\beta\gamma}) + k_{off}}$, where $k_{\beta\gamma}$ is the rate of association between the weakly-bound IL-2/IL-2R α complex and the IL-2R β and IL-2R γ subunits, k_{off} is the rate of dissociation for the IL-2/IL-2R α complex, and $(\#mol_{\beta\gamma})$ is the number of IL-2R β / IL-2R γ . Hence,

$$P_{auto-signaling} = P_{auto-binding} \times \frac{k_{\beta\gamma}(\#mol_{\beta\gamma})}{k_{\beta\gamma}(\#mol_{\beta\gamma}) + k_{off}}.$$

In our system, we estimated $k_{\beta\gamma}=3.3e-4/s$, $k_{off}=0.4/s$ (Figure 2) and the number of free $\beta\gamma$ subunits to be on average 300 molecules per cell (SOM #2C). Hence we estimate the probability of autocrine signaling to be smaller than 10% such that the predominant mode of signaling is clearly paracrine.

By applying the above theory to the model presented by (Busse *et al*, 2010), we find the probability for autocrine signaling to range from 0.0025 to 0.71 when varying the receptor number from 10 to 10,000 receptors. However, there are two discrepancies in Busse *et al.*' model. First, the maximum number of functional receptor complexes should be limited to 1000 molecules due to the limited number of IL-2R β and IL-2R γ receptor chains (cf Figure 2 & 3). Second, the cytokine diffusion coefficient was taken to be:

$$D_{IL-2}(Busse)= 36000 \mu m^2/hr = 10 \mu m^2/s,$$

while theoretical estimates(Berg, 1993) and experimental measurements(Economou *et al*, 1978) yield a faster value of:

$$D_{IL-2} = 100 \mu m^2/s.$$

Calculating the autocrine signaling probability using these experimentally-validated parameters reduces the maximal value for the probability of autocrine signaling to 0.11. For that reason, we argue that in our experimental settings, autocrine signaling is negligible. We confirmed this theoretical insight with the experiments presented in Figure 6A. Consequently the documented IL-2-dependant regulation of T cells must work in a paracrine / quorum sensing mode and not an autocrine mode.

2) Theoretical arguments for a well-mixed model of our experimental system.

Following the theory presented in (Batsilas *et al*, 2003; Berezhkovskii *et al*, 2004), the cumulative probability of a paracrine signal to act at a distance r away from its point of secretion can be well approximated by the expression

$$P(r) \approx \frac{r}{r + 1.1D_L / \kappa_{eff}},$$

with $\kappa_{eff} = \frac{\kappa\sigma}{1 + \pi Da / 4}$, σ being the fraction of the surface being occupied by cells. We will use this approximation to justify some of the geometric approximations that we made in our model of IL-2 paracrine signaling.

We begin by evaluating the distribution of trapping distances for our experiments. We are using 96 well plates with 100,000 cells and 150 μ l of medium. The radius of a single well is 3 mm such that the height of the medium is equal to 5.3 mm. When having 100,000 cells in the medium, about 27% of the surface area covered with cells. Assuming that the cells have 100,000 receptors on their surface, the effective trapping rate constant

is equal to $\kappa_{eff} = 18.75\sigma$, where σ is the fraction of the surface being occupied by cells; thus, 90% of the paracrine signal acts in a region of radius $r_{paracrine} = 400\mu m$ around the point of secretion. This region is orders of magnitude larger than an individual cell justifying our approach to not spatially resolve individual cells but treating them as point particles instead.

One more argument justifies our use of a well-mixed approximation for IL-2 regulation. The density of cells in our experiment is such that their average separation is typically $s=30\mu m$. The timescale for secreted IL-2 to diffuse this distance is $\tau_{diffusion} = s^2/2/D_{IL-2} = 5s$. Considering that the characteristic timescales for IL-2 binding, signaling and depletion is in the minute range, diffusion of IL-2 is not a limiting step and spatial inhomogeneities in IL-2 regulation are most likely negligible in our experimental setting.

SOM #9. Experimental validation of the well-mixed approximation for IL-2

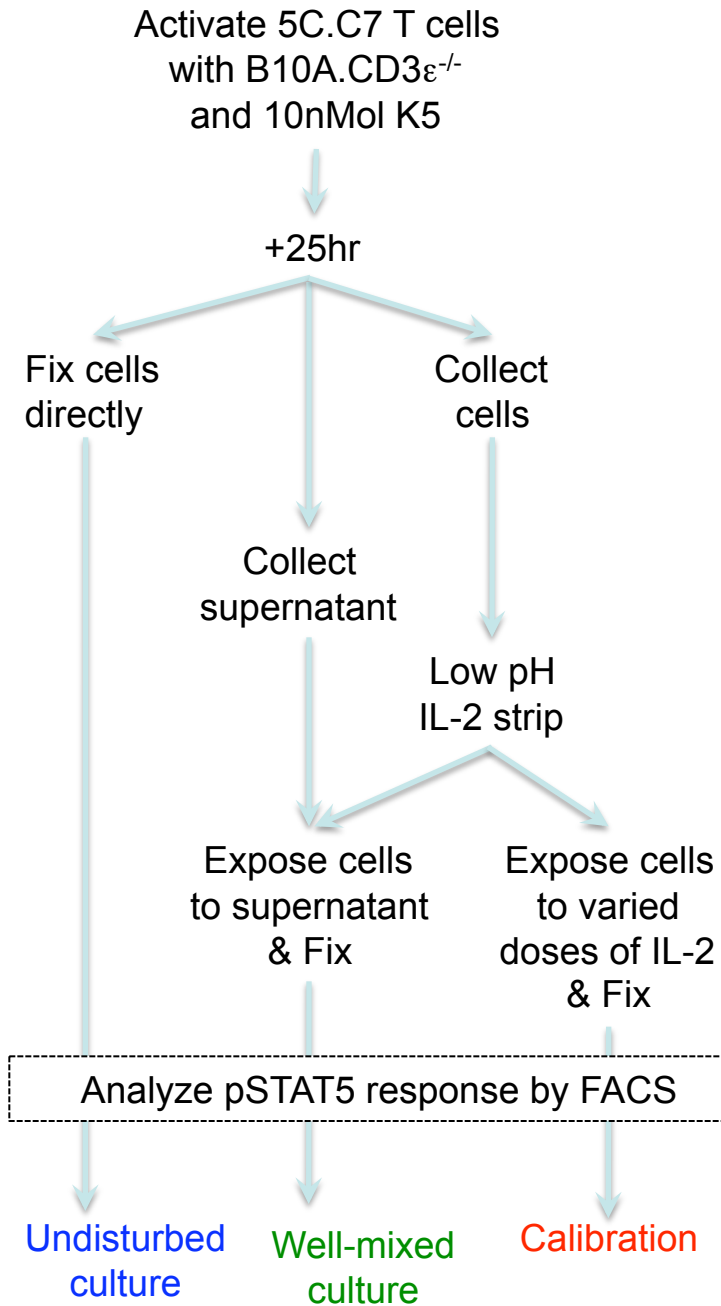
Our computer model assumes a well-mixed environment for the supernatant, based on theoretical arguments presented in SOM #8. Here, we validate this approximation experimentally by comparing the pSTAT5 response for undisturbed cells in culture in our experimental settings with the pSTAT5 response of very same cells after mixing of the supernatant.

5C.C7 TCR-transgenic Rag2-knock-out T cells were activated in vitro with B10.A/CD3e-knock-out splenocytes and 1 μ Mol K5 peptide (see Material & Methods for details). After 25hr of stimulation in vitro, three measurements were performed (Figure SOM #9A). First, cells were fixed immediately in the culture dish: these are our undisturbed cells. Second, the supernatant from this cell culture was harvested and kept for further analysis. Cells from these wells were harvested, stripped of their bound IL-2 with a low-pH solution, and rested for 10min at 37°C to bring down pSTAT5 to basal levels. These cells were then stimulated with the mixed collected supernatant (this is our “well-mixed” culture) or stimulated with varied concentrations of IL-2 for calibration of their pSTAT5 response.

The three samples were processed in parallel to analyze their pSTAT5 response (see Material & Methods for details). We gated on CD4⁺Vb3⁺IL-2R α ^{intermediate} to analyze the pSTAT5 response among activated T cells. In Figure SOM #9B, we found that cells from undisturbed and well-mixed cultures have similar pSTAT5 levels (in between the calibration samples with no IL-2 or excess IL-2). Using the calibration dose response, we back-calculated that the pSTAT5 profile in the undisturbed culture corresponded to an apparent concentration of IL-2 of 20 \pm 5pMol, while the well-mixed cells yielded a pSTAT5 profile that corresponds to an apparent concentration of IL-2 of 17 \pm 5pMol. Hence, the apparent concentrations of IL-2 as sensed by T cells in the undisturbed setting or in the well-mixed settings are identical within error bars. We conclude that the pSTAT5 profile of T cells in our experimental setting (“undisturbed”) is identical to the profile of a well-mixed culture. This validates experimentally the well-mixed approximation for our model.

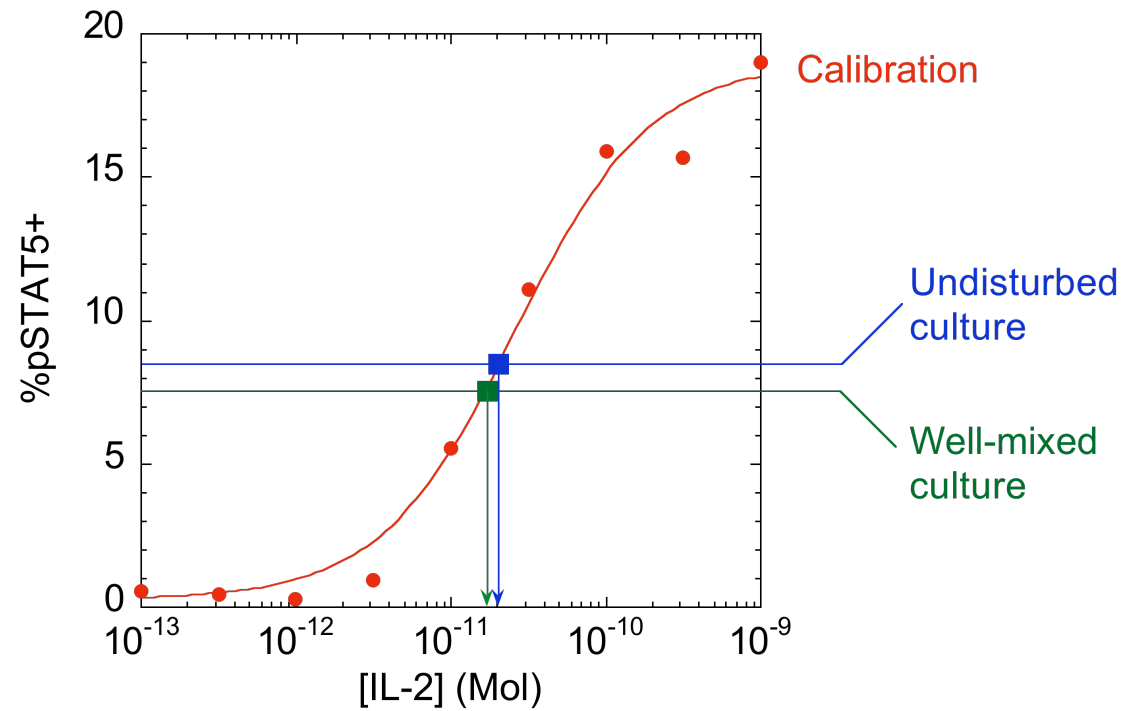
Note that our IL-2R α ^{intermediate} gate selects for activated T cells whose EC₅₀ in IL-2/pSTAT5 response is at 10pMol (Figures 2 and SOM #9B). Gating on IL-2R α ^{hi} cells selects activated T cells whose EC₅₀ is below 1pMol: given our estimate of the concentration of IL-2 in this culture (around 20pMol), these IL-2R α ^{hi} cells have a saturated pSTAT5 response that does not allow us to compare undisturbed and well-mixed cultures.

Figure SOM #9



A

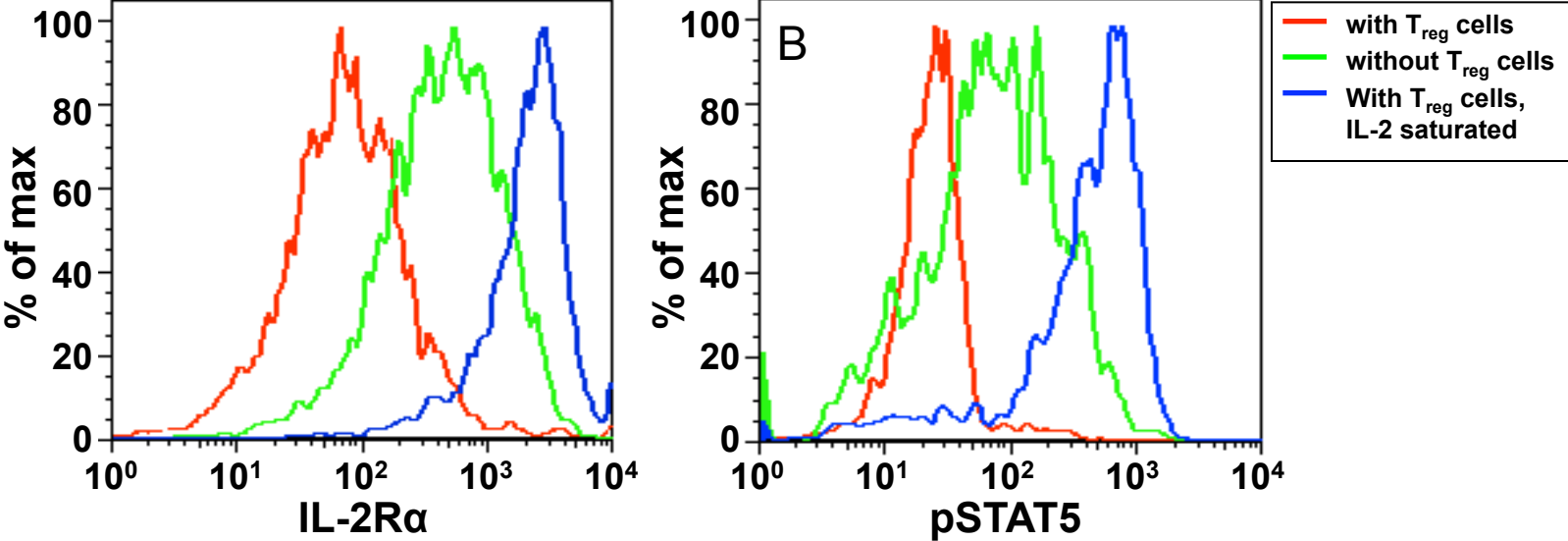
B



SOM #10. Exogenous IL-2 reverses the effect of T_{reg} cells in an α CD3/ α CD28 suppression assay

We show here that exogenous IL-2 reverses the effect of 8×10^4 T_{reg} cells on 10^4 T_{eff} cells following 64 hours of coculture in the presence of α CD3/ α CD28. Suppression on both IL-2R α levels (Figure SOM #10A) and STAT5 phosphorylation (Figure SOM #10B) is reversed.

Figure SOM #10



SOM #11. “The double hit”: T_{reg} cells abrogate IL-2 binding by T_{eff} cells by reducing both IL-2 concentrations and IL-2R α levels in T_{eff} cells under activation with α CD3/ α CD28 cross-linking.

Here we used the classical assay of α CD3/ α CD28 stimulation in a co-culture of T_{reg} and T_{eff} cells (Pandiyani *et al*, 2007; Thornton and Shevach, 1998) to probe how IL-2 depletion correlates with the suppressive capabilities of T_{reg} cells .

Upon α CD3/ α CD28 stimulation, both T_{eff} and T_{reg} cells up-regulate IL-2R α . Moreover, IL-2R α levels on both cell types increase with larger number of effectors as these can be expected to produce larger (total) amounts of IL-2 that markedly amplify IL-2R α up-regulation (Figure SOM #11A). However, we found that for different numbers of effector cells, IL-2R α levels on the T_{reg} cells remained consistently ten-fold higher than those on T_{eff} cells. Our results (Figure 2 & 3) predicted that, in this assay, T_{reg} cells would then be better scavengers for IL-2.

To quantify the IL-2 depletion by T_{reg} cells, we then compared two types of cell cultures: T_{eff} cells alone undergoing activation by α CD3/ α CD28 cross-linking, or T_{eff} cells undergoing activation by α CD3/ α CD28 cross-linking in the presence of T_{reg} cells (purified CD4⁺CD25⁺ cells). We found that T_{reg} cells indeed depleted the medium of the secreted IL-2 and decreased extracellular IL-2 concentrations consistently by five-fold (Figure SOM #11B) at 36 or 64 hours.

In turn, we found that lower IL-2 concentrations in the medium further disrupted the positive feedback by which IL-2 binding leads to the up-regulation of IL-2R α expression (Kim *et al*, 2006). In particular, at intermediate times, *i.e.* around 36h, T_{eff} cells that were cultured with T_{reg} cells exhibited decreased levels of IL-2R α (Figure SOM #11C) compared to T_{eff} cells that were cultured alone. This effect was completely reversed by exogenous addition of a receptor saturating concentration of 100pM of IL-2 (SOM #10).

Similar to the peptide stimulation suppression protocol (figure 5J-K), we compared STAT5 phosphorylation in effector subpopulations with equal IL-2R α expression levels (as defined in Figure SOM #11C), in the presence or absence of T_{reg} cells. In the presence of T_{reg} cells, STAT5 phosphorylation is diminished for intermediate levels of IL-2R α (Figure SOM #11D2,3). This effect becomes less marked for cells with either high (Figure SOM #11D4, all cells are signaling) or low IL-2R α levels (Figure SOM #11D1, no signal in both cultures). This behavior is consistent with the reduced IL-2 levels in the presence of T_{reg} cells.

This IL-2R α /IL-2 composite “double-hit” effect leads to a marked reduction in pSTAT5 levels in T_{eff} cells when cultured with T_{reg} cells (Figure SOM #11E). This reduction of STAT5 phosphorylation at the population level eventually results in increased apoptosis of T_{eff} cells and leads irrevocably to decreased cell numbers at longer time scales (~6 days); T_{eff} cells proliferate 9.1 \pm 2.2 times (Geometrical mean \pm standard error, N=8) more if T_{reg} cells are absent. As previously demonstrated (Pandiyani *et al*, 2007), this long term effect was also completely reversed by the addition of saturating concentrations of exogenous IL-2 (1 nMolar) –cf SOM Figure 10.

Thus, IL-2 depletion by T_{reg} cells reduces both IL-2 concentrations and effector cell sensitivity to IL-2; that induces a drastic decrease of STAT5 phosphorylation in T_{eff} cells.

In Figure SOM #11 we show that:

A. IL-2R α levels on α CD3/ α CD28 stimulated T_{eff} cells (activated cells only) and T_{reg} cells for different numbers of effector cells after 39 hours of coculture. T_{reg} cells consistently express ten-fold more receptors.

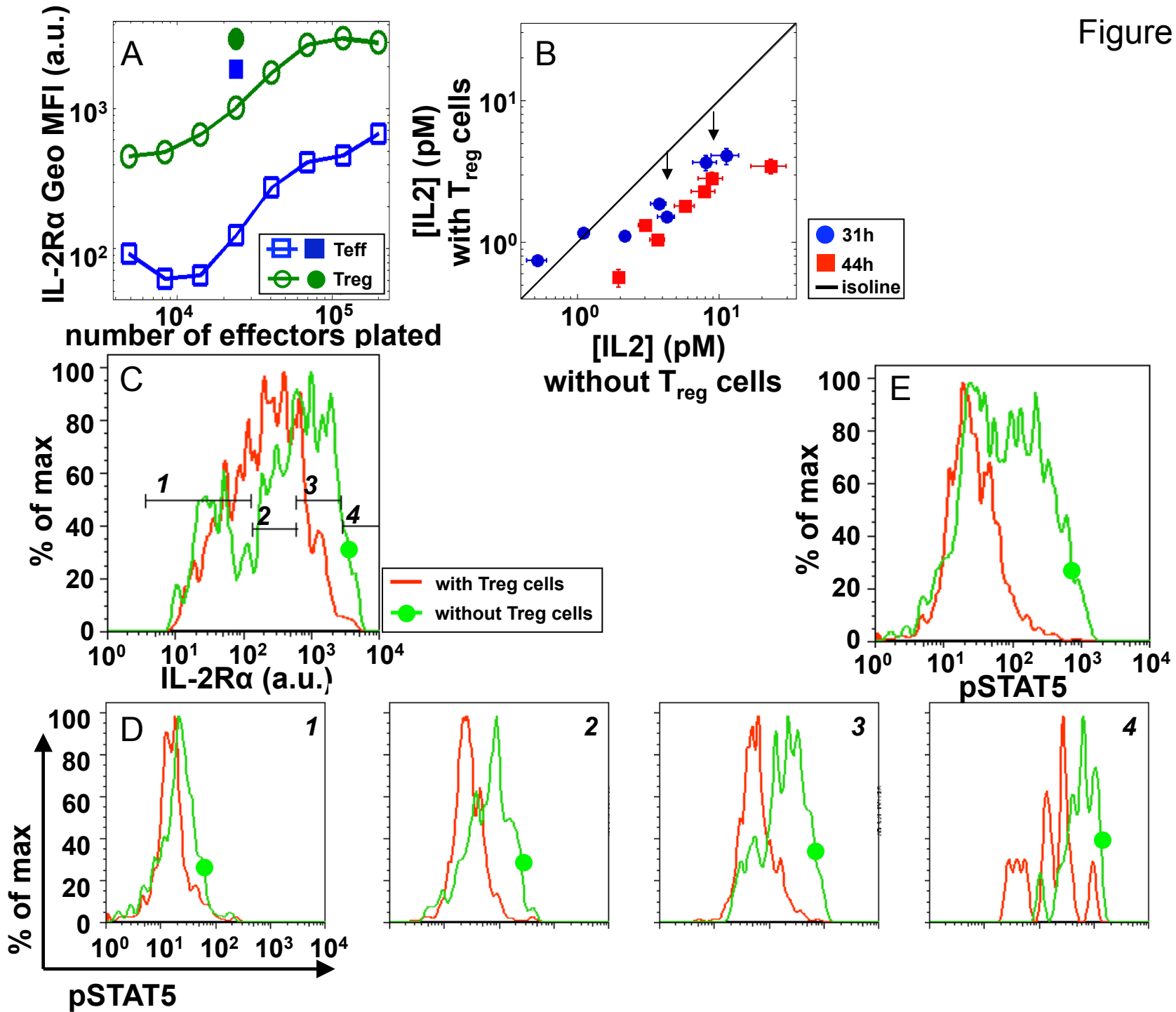
B. Cultures that include T_{reg} cells have reduced IL-2 concentrations, error bars that are not shown are smaller than the symbol.

C. Coculturing $3 \cdot 10^4$ T_{eff} cells with $8 \cdot 10^4$ T_{reg} cells for 39 hours leads to a reduction in IL-2R α expression on the effector cells. This effect is completely reversed by exogenous addition of 1nMolar IL-2 (see SOM #10) confirming that IL-2 consumption by T_{reg} cells disrupts a critical positive feedback loop of IL2 onto IL-2R α in T_{eff} cells.

D. pSTAT5 histograms for the four subpopulations with varied levels of IL-2R α (1-4) as marked in (C) for effector cells or effector cells cocultured with T_{reg} cells. Subpopulations with equal IL-2R α levels show decreased pSTAT5 signaling in the presence of T_{reg} cells, consistently with the decrease concentration of available IL-2.

E. pSTAT5 histograms of the entire two populations. The combined effect of lowered concentrations of IL-2 and lowered IL-2R α levels leads to a marked decrease in pSTAT5 signaling. This downregulation of pSTAT5 is fully reversed by exogenous addition of 1nMolar of IL-2 (see SOM #10).

Figure SOM #11

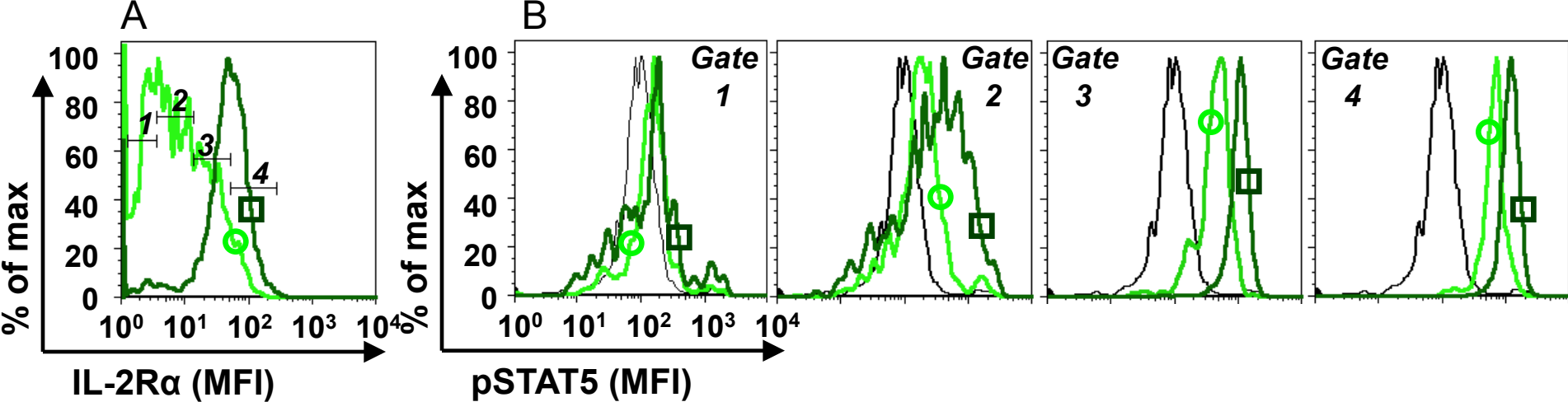


SOM #12. “The double hit”: T_{reg} cells abrogate IL-2 signaling by T_{eff} cells by reducing both IL-2 concentrations and IL-2R α levels in T_{eff} cells under antigen activation.

In order to illustrate the composite effect (or “double-hit”) of IL-2 depletion and limitation in IL-2R α upregulation, we compared pSTAT5 in cultures of T_{eff} cells that were weakly activated with antigens, in the presence or absence of T_{reg} cells. Although the IL-2R α distributions were different between the two cultures (IL-2R α is down-regulated in the presence of T_{reg} cells) we could monitor the pSTAT5 response in subpopulations with equal IL-2R α expression (as defined in Figure SOM#12A), *i.e.* with equal sensitivity to IL-2 (cf Figure 2). For intermediate levels of IL-2R α (Figure SOM#12B2-B3), there is a clear reduction in pSTAT5 signaling for cells cultured with T_{reg} cells. This reduction is less marked for cells expressing high levels of IL-2R α (Figure SOM#12B4, all cells phosphorylate STAT5), or for the cells expressing low levels of IL-2R α (Figure SOM#12B1, no signal in both cultures).

These data correspond to the samples presented in Figure 6.

Figure SOM #12



SOM# 13. Pre-exposure to IL-2 *in vivo* increases T_{reg} cells suppression *in vitro*.

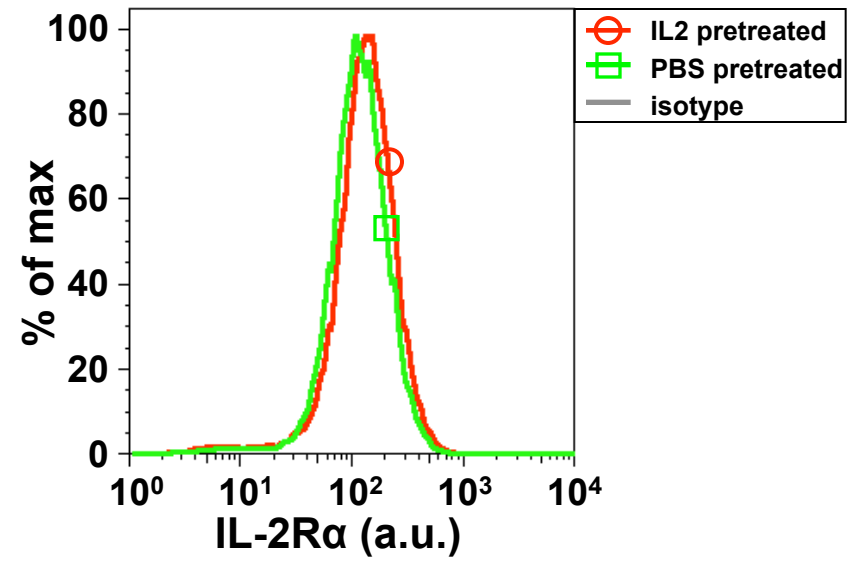
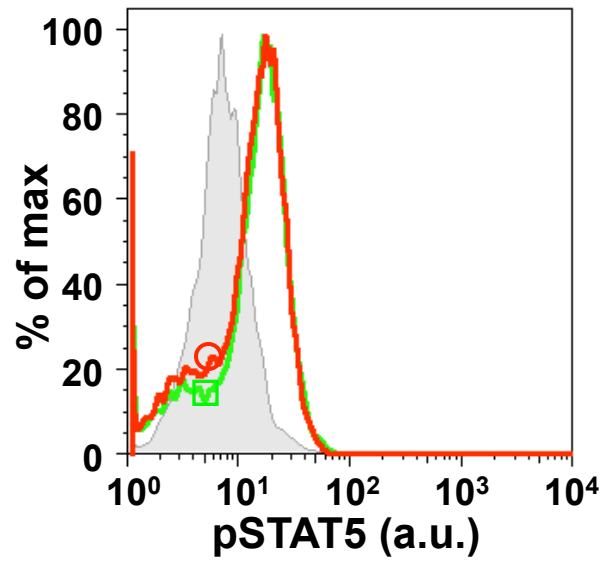
Mice were administered with either IL-2 or PBS injections during 24h (see Methods section). 30hr after the first injection spleens and lymph nodes were harvested and T_{reg} cells isolated using the Miltenyi purification kit (see Methods). 10⁵ T_{reg} cells were then co-cultured *in vitro* with 3*10⁴ 5C.C7 effector cells and 10⁶ B10.A CD3ε^{-/-} pulsed with either 50nM (strong activation) or 1.5nM (weak activation) of K5 peptide. pSTAT5 levels at 47hr (Figure SOM #13A, C) and IL-2Rα levels (Figure SOM #13B, D) at 62hr after plating are presented. When compared to PBS treated cells, we find that T_{reg} cells that were pre-exposed to IL-2 *in vivo* lead to a significant suppression in both of these parameters for weakly activated T_{eff} cells (Figure SOM #13C-D). As expected, there is no evident effect on strongly activated cells (Figure SOM #13A-B) as these can escape T_{reg} surveillance.

Figure SOM #13

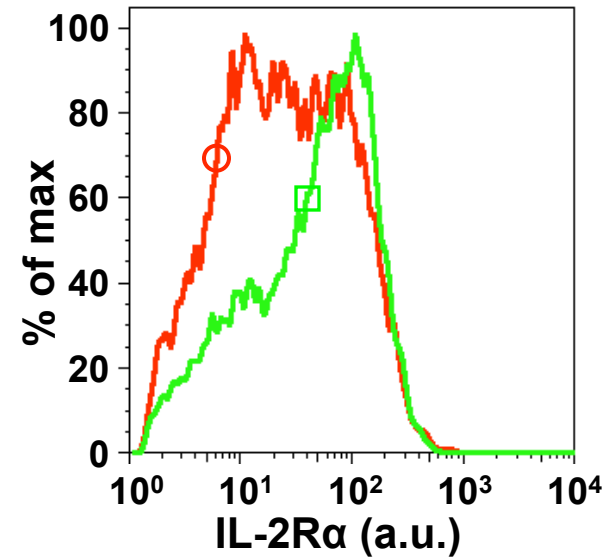
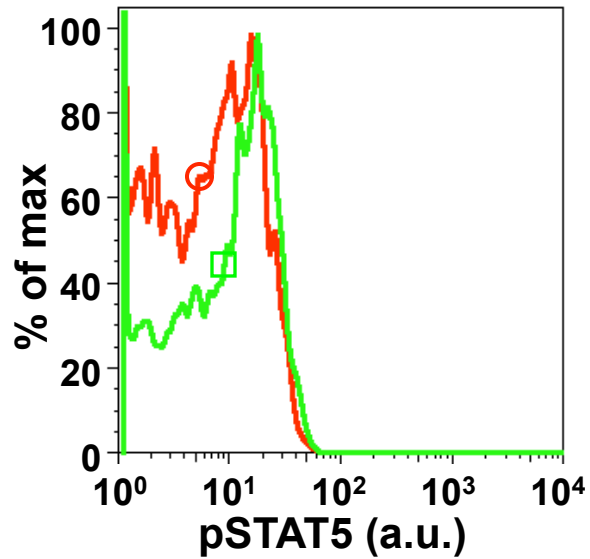
47 hours

62 hours

strong
activation



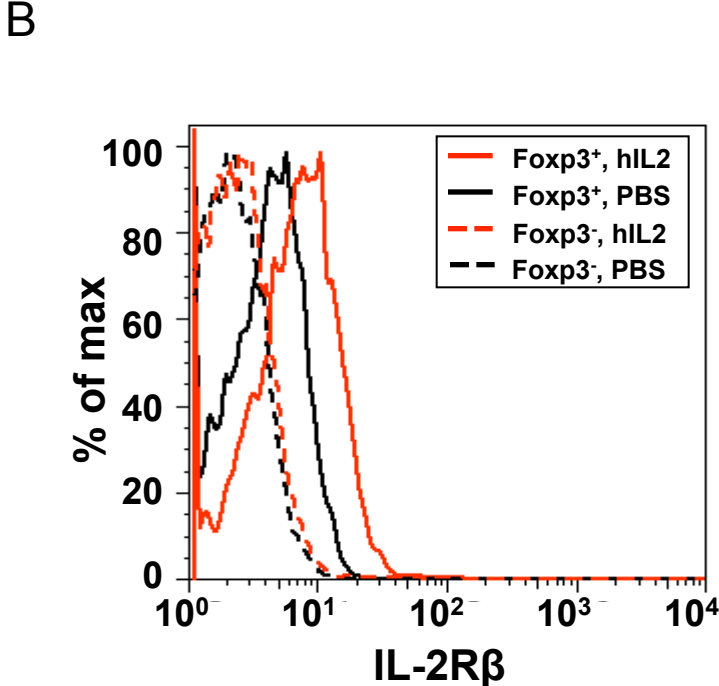
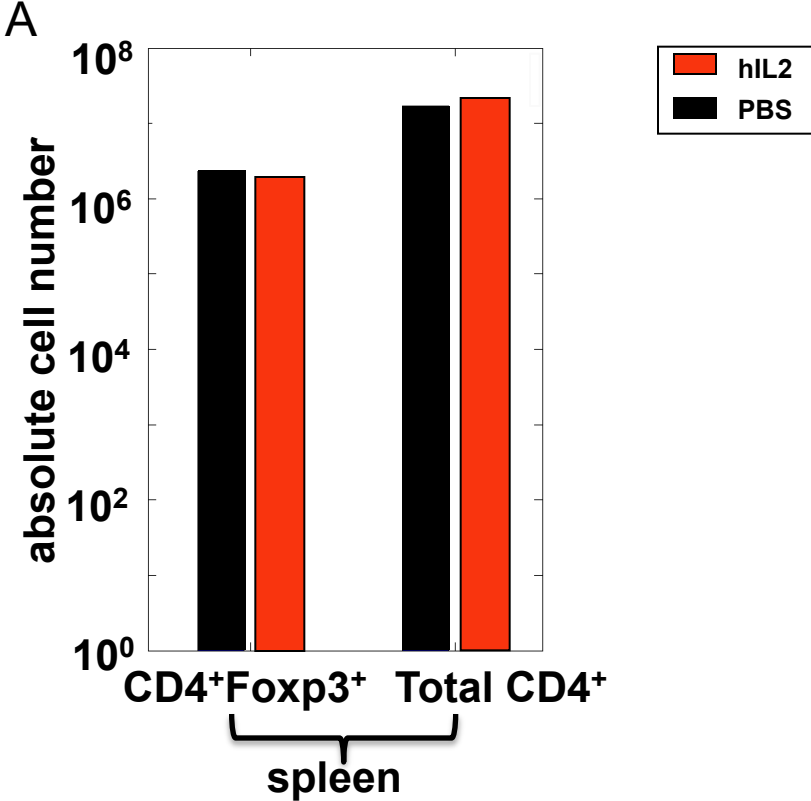
weak
activation



SOM #14. 48hr regimen of IL-2 *in vivo* does not increase the size of the T_{reg} pool.

In Figure SOM #14A, we show that the number of T_{reg} cells in the spleen of mice is not affected by our regimen of intraperitoneal injections of IL2 for 36hr (Figure 7). In Figure SOM #14B, we find that pre-exposure to IL-2 does upregulate slightly the levels of IL-2R β on T_{reg} cells, while the levels of IL-2R α are greatly upregulated (Figure 7B). Overall, exposure to IL-2 *in vivo* does not make T_{reg} cells proliferate or increase in number (at least on this short timescale).

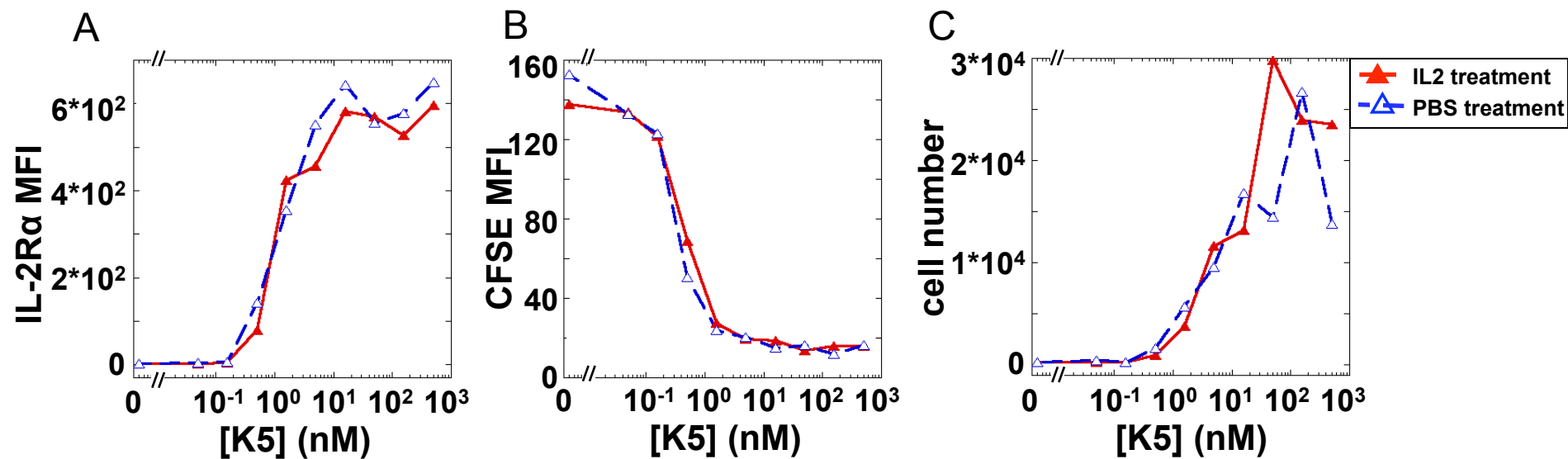
Figure SOM #14



SOM #15. Diminished proliferation after IL-2 injections *in vivo* is not the result of diminished antigen-presenting and activation capabilities by CD4⁻ splenocytes.

Even though the only cells responding *in vivo* to repeated injections of IL-2 are CD25⁺ cells (that are FoxP3⁺ T_{reg} cells in B10.A mice), one needs to check that the limited proliferation of T_{eff} cells *in vivo* (as demonstrated in Figure 7) is not related to a defect in antigen-presentation or any capacity of activation by surrounding cells (e.g. dendritic cells, macrophages or B cells). Thus, we compared the ability of splenocytes from naïve mice treated with 4 intra-peritoneal injections of 1.5µg hIL-2 during 24h, with control mice injected with carrier PBS (these are the conditions used in Figure 7). We used a Miltenyi Bead separation assay to positively select CD4⁻ splenocytes. We then set up an *in vitro* proliferation assay for CFSE-labeled 5C.C7 TCR transgenic Rag2^{-/-} lymphocytes, placed in cultured with these CD4⁻ splenocytes and varied amounts of MCC peptide. IL-2Rα levels (SOM Figure #15A) and proliferation (SOM Figure #15B-C) were measured 64hr after stimulation. These results demonstrate that CD4⁻ splenocytes from IL-2 treated or PBS-treated B10.A mice are identical in their ability to activate 5C.C7 T cells *in vitro*.

Figure SOM #15

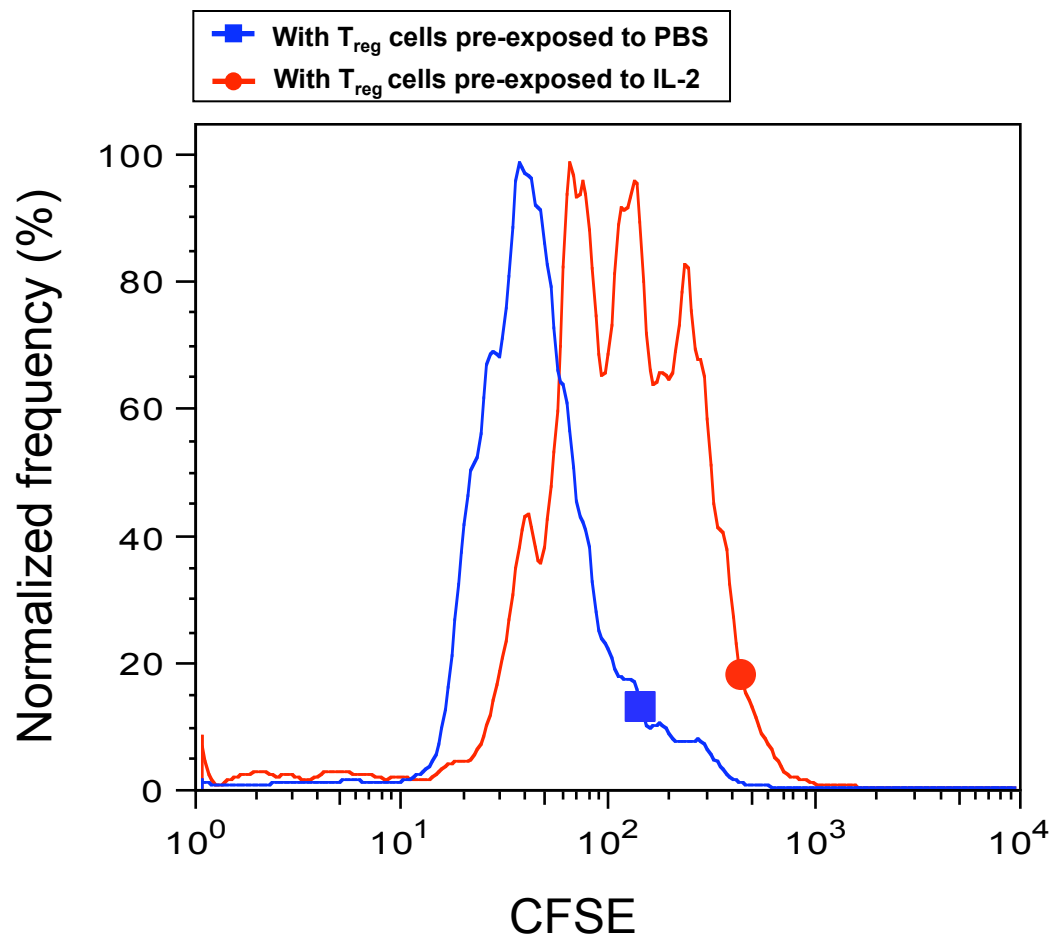


SOM #16. Adoptive transfer of IL-2 treated (compared to PBS-treated) T_{reg} cells is sufficient to limit T_{eff} cell proliferation *in vivo*.

To rule out possible effects (*e.g.* reduced antigen presentation or altered trafficking) of IL-2 administration *in vivo* that may subsequently affect T cell proliferation we used an adoptive transfer strategy to isolate the effect to T_{reg} cells. As detailed in the methods section, T_{reg} cells were purified from the spleen and lymph nodes of mice that had been pretreated with either IL-2 or PBS. These cells (typically one million) were then transferred into B10.A CD3 $\epsilon^{-/-}$ recipients along with one million of CFSE stained naïve 5C.C7 cells and 20 million of B10.A splenocytes to limit homeostatic expansion in such a lymphopenic environment (Dummer *et al*, 2001). Mice were then immunized as in Figure 7A and their spleens harvested 45hr later. The CFSE profiles of T_{eff} cells (gated with anti-CD4 and anti-V β 3 antibody staining) are presented in Figure SOM# 16. Mice that were transferred with IL-2 pre-treated T_{reg} cells substantially limit T_{eff} division. This experiment demonstrates that the suppression effect presented in Figure 7 correlates strictly with the increased suppressive capacities of T_{reg} cells that have undergone IL-2 pretreatment.

Figure SOM #16

T_{eff} cells proliferation after 45hr



SOM References:

Barthlott T, Moncrieffe H, Veldhoen M, Atkins CJ, Christensen J, O'Garra A, Stockinger B (2005) CD25⁺ CD4⁺ T cells compete with naive CD4⁺ T cells for IL-2 and exploit it for the induction of IL-10 production. *Int Immunol* **17**: 279-288.

Batsilas L, Berezhkovskii AM, Shvartsman SY (2003) Stochastic model of autocrine and paracrine signals in cell culture assays. *Biophys J* **85**: 3659-3665.

Berezhkovskii AM, Batsilas L, Shvartsman SY (2004) Ligand trapping in epithelial layers and cell cultures. *Biophys Chem* **107**: 221-227.

Berg HC (1993) *Random walks in biology*, Expanded edn. Princeton, N.J.: Princeton University Press.

Busse D, de la Rosa M, Hobiger K, Thurley K, Flossdorf M, Scheffold A, Hofer T (2010) Competing feedback loops shape IL-2 signaling between helper and regulatory T lymphocytes in cellular microenvironments. *Proc Natl Acad Sci U S A* **107**: 3058-3063.

Cantrell DA, Smith KA (1984) The interleukin-2 T-cell system: a new cell growth model. *Science* **224**: 1312-1316.

de la Rosa M, Rutz S, Dorninger H, Scheffold A (2004) Interleukin-2 is essential for CD4⁺CD25⁺ regulatory T cell function. *Eur J Immunol* **34**: 2480-2488.

Dummer W, Ernst B, LeRoy E, Lee D, Surh C (2001) Autologous regulation of naive T cell homeostasis within the T cell compartment. *J Immunol* **166**: 2460-2468.

Duprez V, Dautry-Varsat A (1986) Receptor-mediated endocytosis of interleukin 2 in a human tumor T cell line. Degradation of interleukin 2 and evidence for the absence of recycling of interleukin receptors. *J Biol Chem* **261**: 15450-15454.

Economou JS, Shin HS (1978) Lymphocyte-activating factor. I. Generation and physicochemical characterization. *J Immunol* **121**: 1446-1452.

Ellery JM, Nicholls PJ (2002) Alternate signalling pathways from the interleukin-2 receptor. *Cytokine Growth Factor Rev* **13**: 27-40.

Feinerman O, Veiga J, Dorfman JR, Germain RN, Altan-Bonnet G (2008) Variability and robustness in T cell activation from regulated heterogeneity in protein levels. *Science* **321**: 1081-1084.

Kim HP, Imbert J, Leonard WJ (2006) Both integrated and differential regulation of components of the IL-2/IL-2 receptor system. *Cytokine Growth Factor Rev* **17**: 349-366.

Kim HP, Kelly J, Leonard WJ (2001) The basis for IL-2-induced IL-2 receptor alpha chain gene regulation: importance of two widely separated IL-2 response elements. *Immunity* **15**: 159-172.

Liparoto SF, Myszka DG, Wu Z, Goldstein B, Laue TM, Ciardelli TL (2002) Analysis of the role of the interleukin-2 receptor gamma chain in ligand binding. *Biochemistry* **41**: 2543-2551.

Pandiyan P, Zheng L, Ishihara S, Reed J, Lenardo MJ (2007) CD4+CD25+Foxp3+ regulatory T cells induce cytokine deprivation-mediated apoptosis of effector CD4+ T cells. *Nat Immunol* **8**: 1353-1362.

Pillet AH, Lavergne V, Pasquier V, Gesbert F, Theze J, Rose T IL-2 Induces Conformational Changes in Its Preassembled Receptor Core, Which Then Migrates in Lipid Raft and Binds to the Cytoskeleton Meshwork. *J Mol Biol.* (2010) in press. PMID: 20816854

Rickert M, Wang X, Boulanger MJ, Goriatcheva N, Garcia KC (2005) The structure of interleukin-2 complexed with its alpha receptor. *Science* **308**: 1477-1480.

Smith KA (1988) Interleukin-2: inception, impact, and implications. *Science* **240**: 1169-1176.

Sojka DK, Hughson A, Sukiennicki TL, Fowell DJ (2005) Early kinetic window of target T cell susceptibility to CD25+ regulatory T cell activity. *J Immunol* **175**: 7274-7280.

Takeshita T, Asao H, Ohtani K, Ishii N, Kumaki S, Tanaka N, Munakata H, Nakamura M, Sugamura K (1992) Cloning of the gamma chain of the human IL-2 receptor. *Science* **257**: 379-382.

Thornton AM, Shevach EM (1998) CD4+CD25+ immunoregulatory T cells suppress polyclonal T cell activation in vitro by inhibiting interleukin 2 production. *J Exp Med* **188**: 287-296.

Villarino AV, Tato CM, Stumhofer JS, Yao Z, Cui YK, Hennighausen L, O'Shea JJ, Hunter CA (2007) Helper T cell IL-2 production is limited by negative feedback and STAT-dependent cytokine signals. *J Exp Med* **204**: 65-71.

Wang HM, Smith KA (1987) The interleukin 2 receptor. Functional consequences of its bimolecular structure. *J Exp Med* **166**: 1055-1069.

Wang X, Rickert M, Garcia KC (2005) Structure of the quaternary complex of interleukin-2 with its alpha, beta, and gammac receptors. *Science* **310**: 1159-1163.

Wu Z, Goldstein B, Laue TM, Liparoto SF, Nemeth MJ, Ciardelli TL (1999) Solution assembly of the pseudo-high affinity and intermediate affinity interleukin-2 receptor complexes. *Protein Sci* **8**: 482-489.

Wu Z, Johnson KW, Goldstein B, Choi Y, Eaton SF, Laue TM, Ciardelli TL (1995) Solution assembly of a soluble, heteromeric, high affinity interleukin-2 receptor complex. *J Biol Chem* **270**: 16039-16044.